

Accepted Manuscript

Title: Experimental investigation and simulation of structure and tensile properties of Tempcore treated rebar

Author: Hany Khalifa G.M. Megahed Rawia M. Hamouda
Mohamed A. Taha



PII: S0924-0136(15)30209-0
DOI: <http://dx.doi.org/doi:10.1016/j.jmatprotec.2015.11.023>
Reference: PROTEC 14640

To appear in: *Journal of Materials Processing Technology*

Received date: 8-4-2015
Revised date: 4-11-2015
Accepted date: 23-11-2015

Please cite this article as: Khalifa, Hany, Megahed, G.M., Hamouda, Rawia M., Taha, Mohamed A., Experimental investigation and simulation of structure and tensile properties of Tempcore treated rebar. *Journal of Materials Processing Technology* <http://dx.doi.org/10.1016/j.jmatprotec.2015.11.023>

This is a PDF file of an unedited manuscript that has been accepted for publication. As a service to our customers we are providing this early version of the manuscript. The manuscript will undergo copyediting, typesetting, and review of the resulting proof before it is published in its final form. Please note that during the production process errors may be discovered which could affect the content, and all legal disclaimers that apply to the journal pertain.

Experimental investigation and simulation of structure and tensile properties of Tempcore treated rebar

Hany Khalifa^a, G.M.Megahed^a,
Rawia M. Hamouda^b and Mohamed A. Taha^{b,*}

^aEZZ steel –Soukna– Egypt.

^bFaculty of Engineering, Ain-Shams University, Cairo – Egypt.

* Corresponding Author, Email: m_ataha@yahoo.com

Highlights

- We develop a mathematical model for simulating the Tempcore process.
- The model consists of three parts, thermal model, metallurgical model and mechanical model.
- The model has been applied to B500B steel bars. Its variables are expressed in terms of chemical composition, and process parameters, namely: bar diameter, rolling temperature, number and setting of cooling nozzles, cooling water flow rate and quenching time.
- It is found that numerically calculated data are in good agreement with those obtained from experimental trials accomplished at EZZ STEEL plant.

Abstract

This paper presents a mathematical model for simulating Tempcore process, the model consisting of three successive parts. Thermal model is used to predict the temperature distribution across the bar over its whole quenching and self-tempering rout. The output of this model is used to calculate the area of martensite formed in outer layer and ferrite – pearlite heart. The composite rule of mixtures (ROM) is used to correlate the tensile yield strength of the bar with the martensite and ferrite-pearlite volume fraction. The model is capable of predicting the effect of various process parameters namely; bar diameter,

rolling temperature, number and setting of cooling nozzles, cooling water flow rate and quenching time on the thermal conditions across the bar during different stages of the process, structure formed and tensile behavior of the rebar .A good agreement is found between the predicted results and the experimental data for B500B steel with diameters from 10 to 16 mm and yield strength varied from 400 Mpa to 700 Mpa .

Keywords: Tempcore process, steel rebar, modeling and simulation of metallurgical processing, heat transfer, martensite, mechanical properties

1. Introduction

Tempcore process consists of three stages, the first stage a bar emerging from last rolling stand is rapidly cooled with water, to form martensite in surface layer. At the second stage heat flows from the center to the surface and a self -tempering treatment of martensite is achieved as demonstrated by Economopoulos et al. (1975).Çetinel et al. (2000) proved that the self -tempering temperature or the equalizing temperature decreases with increasing water flux. Simon et al. (1984) reported that the tempering process ensures the proper ductility of the material, simultaneously preserving its high yield strength. Finally, in the third stage: during the slow cooling of the bar on the cooling bed the austenite core transforms to ferrite and pearlite as broadcasted by Economopoulos et al. (1975).Typical temperature profile at the different stages and the corresponding microstructural changes are illustrated schematically by Daniele Inc.(2010), as indicated in Fig.1.

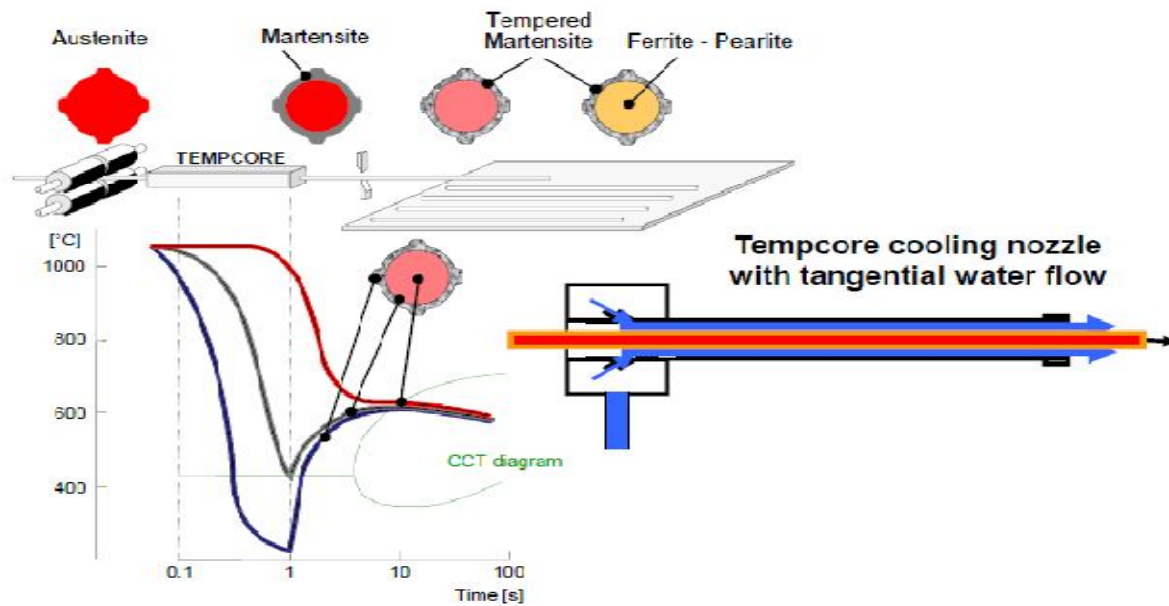


Fig.1: Temperature profile of Tempcore treated bars at the different stages and the corresponding microstructural changes (Daniele Inc., 2010).

Martensite volume fraction, tempering temperature and strength of the Tempcore treated rebar depend on rolling parameters. Hence, these parameters need to be closely controlled so that consistent mechanical properties can be achieved. This prompts the need for a heat transfer model and phase transformation model coupled with a yield strength prediction model, which can then be used to control the rolling parameters so that the desired martensite depth, tempering temperature are achieved. Mathematical models describing heat transfer and phase transformation of alloys during cooling processes have been developed to predict the temperature distribution and fraction of phase transformed during cooling of steel bars, plates and rods. Isukapalli et al.(2010) conducted a mathematical model to Predicted heat transfer coefficient of steel bars subjected to Tempcore process using nonlinear modeling. Çetinel et al. (2000) employed the finite

element to the microstructural evolution of steels subjected to the Tempcore process. Prakash et al. (1981) and Munirae et al. (1994) investigate austenite pearlite transformation in eutectoid carbon steel. Deniset et al. (1992) developed a mathematical model coupled with phase transformation and temperature evolution in steel. Suehiro et al. (1992) applied a mathematical model for prediction of microstructural evolution to high carbon steel. Purcell, (2000) conducted a mathematical model to simulate temperature evolution in the hot rolling of steel bars. Lindemann et al. (2005) developed a mathematical model including the geometrical characterization of wire rod to predict thermal behavior of hot rolled wire rod. Nobari et al. (2011) and Kang et al. (2005) developed a mathematical model based on the finite element method to evaluate coupled thermal metallurgical behavior of steel rods and wires. The general structure of the models includes both temperature evolution of the bar and metallurgical parts. However, a model to predict the strength of rebar as function of the Tempcore process parameters is still lacking. Therefore, the aim of the present work is to develop a model to predict the yield strength of Tempcore treated bars as a function of the water flow, water pressure, water temperature, inside diameter of the tube through which bar travels, diameter of the steel rod, quenching time, and surface temperature of the steel rod as well as chemical composition of the treated bars.

2. Methodology

The interrelationship between the Tempcore processing conditions, the associated thermal conditions, martensite formation and resulted yield strength can be represented by the flow diagram in Fig. 2. Three components are incorporated in the model successively namely; heat transfer, structure formation and tensile yield strength. The

finite difference method is used in the first model component to determine the continuous cooling curves at different locations across the bar from its center to its surface. The equalizing temperature, at which all cooling curves meet, represents the tempering temperature. The data are used in the second model to calculate the martensite volume fraction formed. In the third model part, the composite ROM is used to correlate between the Ms Volume fraction and the yield strength.

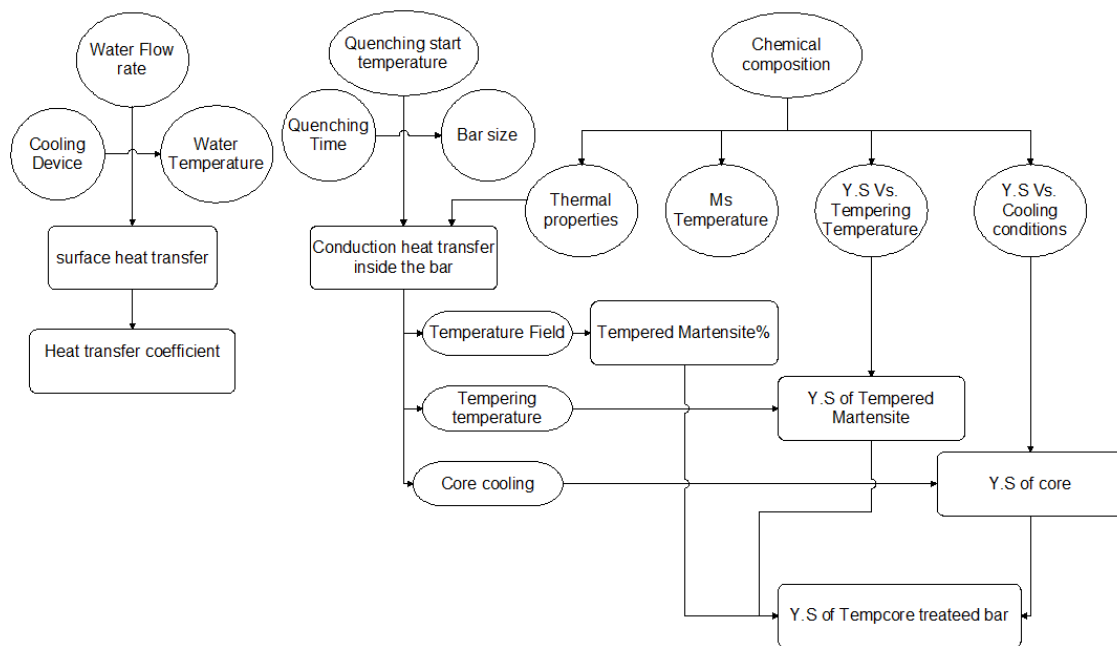


Fig.2: Relation between the process parameters and the main mechanisms of Tempcore process

3. Experimental work

B500B, C-Mn steel bars of 10 mm and 16 mm diameters with chemical compositions as listed in Table 1, which is produced in a steel plant, is used for the investigation in the present work. The measured on-line machine operating parameters are: water flow rate, rolling speed, and rolling temperature. These parameters have been recorded, while the

resulting tempering temperature (TT) was measured. The quenching time (duration of the first stage in which bar is subjected to quenching with water) is then calculated.

Metallographic cross-sectional samples were prepared from the Tempcore rebars, where the polished samples were etched using 3% Nital. Microscopic investigation is used to identify the different microstructural zones across. Room temperature tensile test was used to determine the yield stress.

Table 1: Chemical composition of the investigated reinforcing steels (mass contents in %).

Heat no.	size, mm	C	Si	Mn	P	S	Cr	Ni	Cu	Mo	V	Nb	CE
1	10	0.220	0.159	0.794	0.016	0.020	0.044	0.107	0.419	0.016	0.002	0.001	0.399
2	16	0.229	0.159	0.799	0.022	0.021	0.065	0.108	0.430	0.016	0.002	0.001	0.414
3	10	0.230	0.153	0.765	0.022	0.014	0.092	0.120	0.454	0.011	0.002	0.001	0.416
4	10	0.261	0.175	0.723	0.012	0.015	0.056	0.068	0.273	0.015	0.002	0.002	0.418
5	10	0.255	0.133	0.706	0.008	0.021	0.050	0.050	0.198	0.008	0.002	0.001	0.418
6	16	0.255	0.147	0.626	0.010	0.014	0.039	0.064	0.252	0.009	0.002	0.001	0.401
7	16	0.228	0.150	0.781	0.020	0.016	0.086	0.077	0.264	0.013	0.002	0.001	0.401

4. Mathematical model

The integrated model was developed using C # .net programming language which simulates the cooling of Tempcore treated bars; describes the thermal history across the bar, the percent of area cooled under martensite formation temperature, and the tensile properties of the bar under different settings of Tempcore process parameters. This has

been achieved through three main model parts. The first part is the thermal model which describes the thermal history across the bar during the cooling. The second part is the metallurgical model, which determines the percentage of martensite volume fraction and the core volume fraction. The third part is the mechanical model which predicts the tensile properties of the bar based on the calculation resulted from the previous model.

4.1. Thermal model

In this part, the heat flow and temperature distribution across the bar is described along the whole cooling process from the entry of the cooling box and continuing till bar achieves equalizing temperature at cooling bed. Models describes heat flow inside the quenching box was developed using the FDE (finite difference equations). Also the same technique is used to describe the heat flow in air from quenching box exit to the equalizing temperature achieved at the cooling bed. The model has been formulated for the case of an infinitely long steel bar moving through the cooling box. Allen, 2011 confirmed that in such this case axial heat conduction can be ignored because it is negligible compared to the bulk radial flow of the heat and also because the axial temperature gradient along the bar is small. Fig.3 presents the type of heat transfer problem being modeled, one dimensional, cylindrical, and transient conduction problem. The following assumptions have been considered in the model:

- Uniform initial temperature, which is the rolling finishing temperature of last stand.
- Radial symmetry about the bar centerline.
- Independence of temperature on angular displacement.

- Uniform circular cross section.

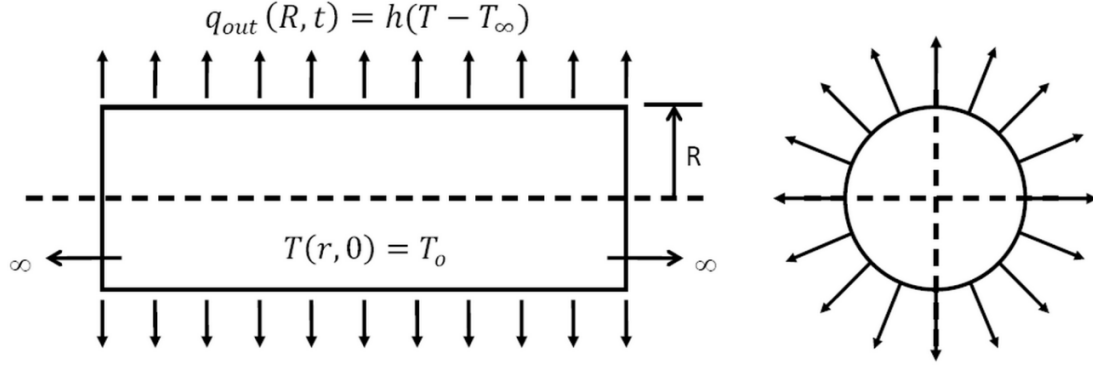


Fig.3: One-dimensional heat transfer in infinite cylinder

The thermal model based on the numerical solution of the following non steady conduction heat transfer equation 1, in order to determine the temperature distribution across the bar cross section with time.

$$\frac{\partial}{\partial r} \left(k \frac{\partial T}{\partial r} \right) + \frac{k}{r} \left(\frac{\partial T}{\partial r} \right) = \rho C_p \frac{\partial T}{\partial t} \quad 1$$

Where ρ , C_p , and k are the density, the specific heat, and the conductivity of the material respectively and t is the time (Holman, 1990).

Boundary Conditions

At the bar cross-section Center:

$$\frac{\partial T}{\partial r} \Big|_{r=0} = 0 \quad 2$$

At the bar surface:

$$-k \frac{\partial T}{\partial r} \Big|_{r=R} = h[T(r, t) - T_{\infty}] \quad 3$$

Where:

T_{∞} is the temperature of the adjacent fluid and h which is the convection coefficient.

h : is the convective heat transfer coefficient between water and the bar

Heat transfer coefficient of water during the entire cooling stage is calculated by equations 4 and 5 in case of $Re < 5000$ and in case of $Re \geq 5000$ respectively (Holman, 1990).

$$h = \frac{\{(1.86)(Re.pr)^{0.33}.k_w\}}{Dh} \quad 4$$

$$h = \frac{\{(0.023)(Pr)^{0.3}(Re)^{0.8}\}}{Dh} \quad 5$$

Where:

Dh : is hydraulic diameter calculated as $(Dh = \frac{4A}{p})$, p is the wetted perimeter $(p=2\pi \frac{(Rc+R)}{2})$.

Pr : is Prandtle number.

k_w : is Thermal conductivity.

Re : is the Renolds number and is calculated as shown in equation 6

$$Re = \frac{(V \text{ relative } \times \rho \text{ water } \times Dh)}{\nu} \quad 6$$

Where:

ν = dynamic viscosity of the water

ρ_{water} = water density

V_{relative} is the relative velocity between water and the quenched bar.

Water velocity will be equal to the flow rate per nozzle divided by the area of the boundary water cooling which, in this case, is the difference in area between the pipe and the rolled bar as described by:

$$V_{\text{water}} (\text{water velocity}) = \frac{Q_{\text{per nozzle}}}{A} \quad , \quad 7$$

$$Q_{\text{per nozzle}} = (\text{flow rate per nozzle}) = \frac{\text{Total flow rate for the quenching box line}}{\text{Number of active nozzles in service}} \quad 8$$

$$A = \text{Area} = A = \pi \{ (R_c)^2 - (R)^2 \} \quad 9$$

Where:

R_c = radius of cooling pipe.

R : the quenched bar diameter size

$$V_{\text{Relative}} = |v_{\text{water}} - v_{\text{bar}}| \quad 10$$

V_{bar} = the bar linear velocity; input independent parameter to the model taken from the rolling mill speed control human machine interface HMI.

Initial Conditions:

The model assumes that the initial temperature is uniform (T_{initial}) through the diameter of the bar.

4.2. Discretization

The first step, which applies the finite difference method, is to divide the geometry of the cylinder into small segments. As indicated in [fig.4](#), a cylinder is divided into segments using concentric rings. At the centre of each segment, a node is defined representing the point for which a value will be calculated. Since the heat transfer problem being solved is one-dimensional, therefore the temperature throughout the cylinder is dependent only on the radial dimension (i.e. the distance from the center of the bar). This means that the discretization can be simply represented by a single node for each radial segment as shown to the right in Fig.4. The thickness of each segment, Δr , is similar throughout the cylinder with the exception of the surface and centre segments. These areas require special consideration. Because heat transfer between the cylinder and surrounding fluid occurs at the surface. To more accurately determine the thermal conditions in this region of the cylinder, this node is assigned a thickness half of that of the interior nodes ($\Delta r/2$). Also, since there is a boundary condition at the centre of the cylinder, a node is required at that point. Because the centre is symmetric, using a thickness of $\Delta r/2$ will actually result in a central nodal segment equal to Δr .

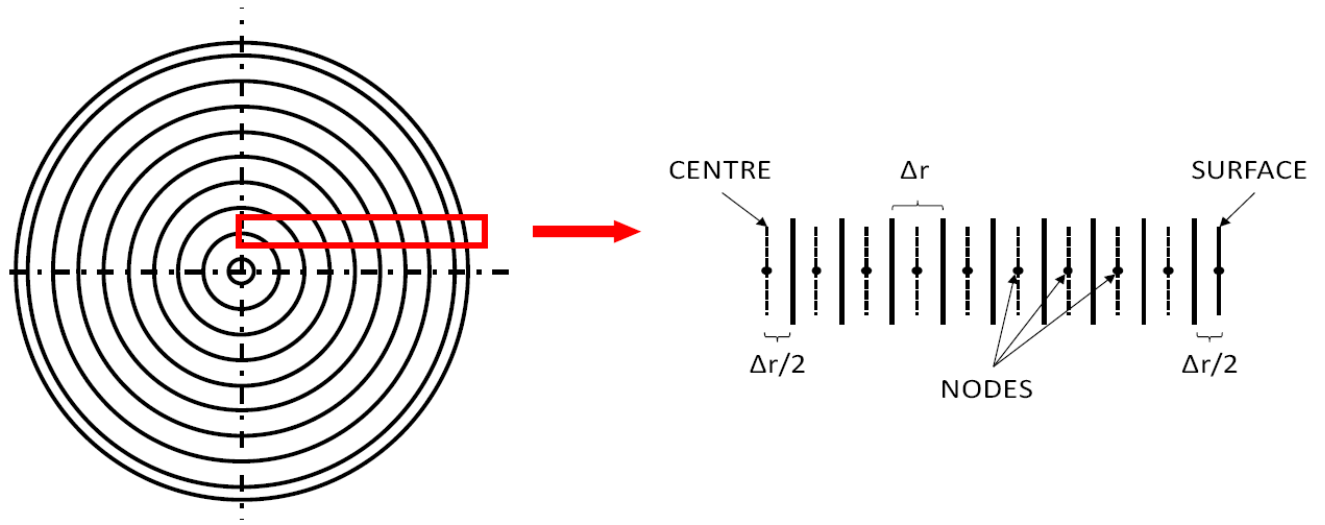


Fig.4: Discretization of Cylinder

4.3. Explicit Form of FDE

Heat balances were made for three different types of nodes existing in the bar cross section, which are namely, the surface node (boundary node), the centerline node, and the general internal node are calculated according to the following equation.(Incropera ,1996)

$$\sum E_{in} + E_g = \Delta v \rho C_p \left(\frac{T^{t+\Delta t} - T^t}{\Delta t} \right) \quad 11$$

Where, E_{in} is the heat entering to the node and E_g is the internal heat generation.

Where: Δv is the volume of the node in m^3 and Δt is the time step in seconds.

Then the solution for the nodal temperature at time t which is mentioned as (T^t) of node i and adjacent nodes for each type of nodes is as follows:

For the boundary node $r=R$:

$$T^{t+\Delta t} = \frac{\Delta t}{\rho C_p} \left[\left(\frac{2k}{\Delta r^2} - \frac{k}{R\Delta r} \right) T_2^t + \left(\frac{2h}{\Delta r} \right) T_{\text{water or air}} + \left(\frac{\rho C_p}{\Delta t} - \left(\frac{2k}{\Delta r^2} - \frac{k}{R\Delta r} \right) - \frac{2h}{\Delta r} \right) T^t \right] \quad 12$$

For center line node: $r=0$

$$T^{t+\Delta t} = \frac{\Delta t}{\rho C_p} \left[\left(\frac{4k}{\Delta r^2} \right) T_1^t + \left(\frac{\rho C_p}{\Delta t} - \frac{4k}{\Delta r^2} \right) T^t \right] \quad 13$$

For general node $0 < r < R$

$$T^{t+\Delta t} = \frac{\Delta t}{\rho C_p} \left[\left(\frac{k}{\Delta r^2} \right) (T_1^t + T_2^t) + \left(\frac{k}{2R\Delta r} \right) (T_1^t - T_2^t) + \left(\frac{\rho C_p}{\Delta t} - \frac{2k}{\Delta r^2} \right) T^t \right] \quad 14$$

Where, T_1 is the temperature of adjacent node toward the surface direction and T_2 the temperature of adjacent node in the direction of the center line.

4.4. Stability equations

For the boundary node $r=R$:

$$\Delta t \leq \frac{\rho C_p \Delta r^2}{4k} \quad 15$$

For center line node: $r=0$

$$\Delta t \leq \frac{\rho C_p \Delta r^2}{2k} \quad 16$$

For general node $0 < r < R$

$$\Delta t \leq \frac{\rho C_p \Delta r^2}{\left[\left(\frac{2k}{\Delta r^2} \right) - \left(\frac{k}{R\Delta r} \right) + \left(\frac{2h}{\Delta r} \right) \right]} \quad 17$$

In the model, Δt has been calculated from three stability equations for boundary, centerline and general node, then the minimum has been utilized in the model run calculation to ensure the stability of the solution. Heat transfer coefficient used in time stability calculation is water heat transfer coefficient where the change in temperature is very quick more than the air heat transfer coefficient. Figure 5 shows thermal profile during quenching and self-tempering stages.

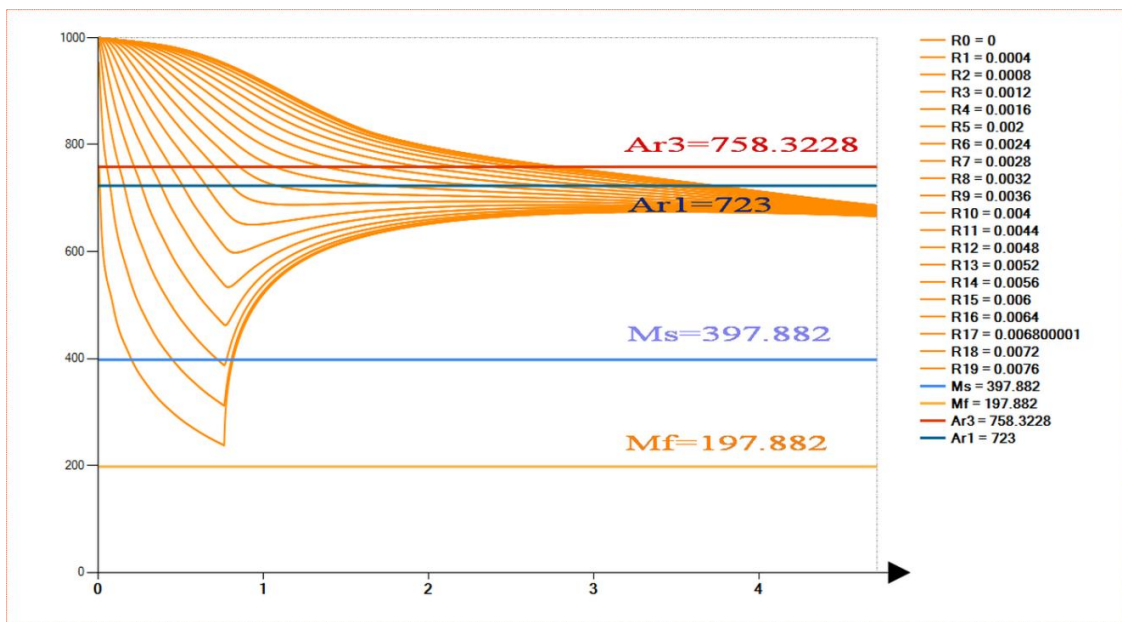


Fig.5: Thermal profile of the bar from the cooling box entering to equalizing temperature normal scale.

4.5. Metallurgical model

The solution of the heat conduction with convection heat transfer boundary conditions in the previous model enables the calculation of temperature at any moment at any point of the cross section of the bar. Having thus determined the thermal field in the bar, therefore it is possible to calculate the Volume percentage of martensite V_M which is an important parameter in Tempcore process since it affects the final mechanical properties of the bar.

Fig. 6 shows the temperature distribution in a cross section of a 16 mm diameter bar after 1 seconds of quenching divided to 200 intervals.

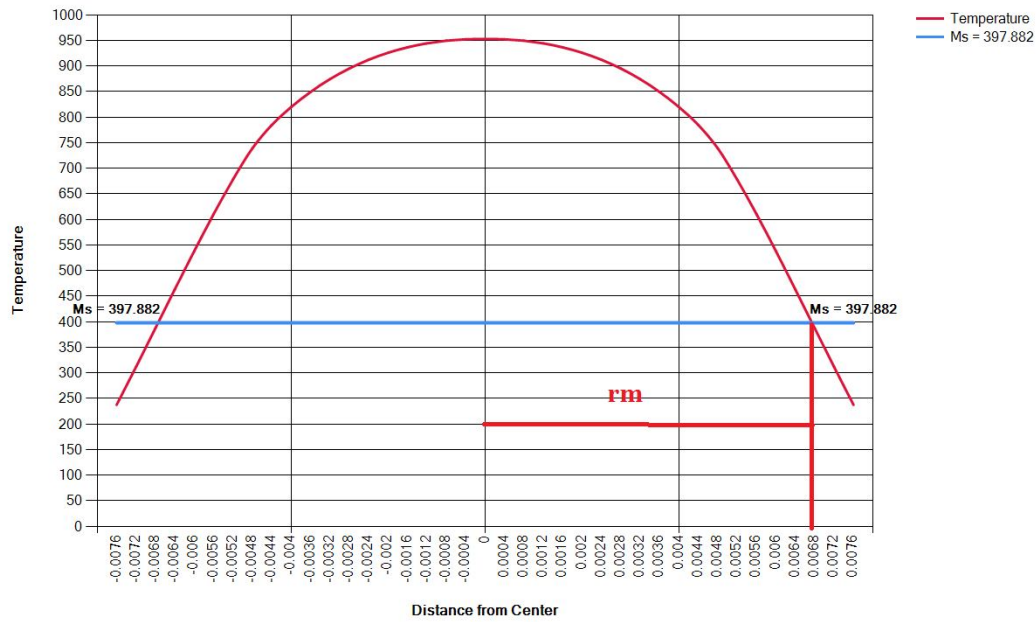


Fig.6: Thermal profile of a bar at exit from cooling box time at quenching durations 1 second.

The volume percentage of martensite V_M depends on the starting temperature of martensite transformation M_s point; is a function of a chemical composition of the bar according to the following equation (Purcell, 2000).

$$M_s = -361(c\%) - 39(Mn\%) + 500 \quad 18$$

The model predict the depth of region cooled under martensite start temperature M_s for the temperature profile of the cross section of the bar at the moment bar leaves the cooling box . Therefore the martensite volume fraction is expressed by the relation shown in the following equation.

$$V_{M=100} \left[1 - \left(\frac{r_m}{D} \right)^2 \right] \quad 19$$

Where V_M is martensite volume fraction, r_m is the distance of martensite layer from center.

4.6. Mechanical properties model

The mechanical behavior at room temperature of the final product with a mixed microstructure is a function of the strength, the distribution and the volume fraction of each micro-constituent. Rodríguez et al, (2004) studied yield strength of the mixed microstructure based on rule of mixtures as shown in the following equation.

$$Y.S_{mix} = \sum V_i * Y.S_i \quad 20$$

Where:

$Y.S_{mix}$, $Y.S_i$ are respectively the yield strength of the material and yield strength of each individual constituent.

V_i , is the volume percentage of each individual constituent

Calculation of Y.S of Tempcore treated bars, was based on the regression data taken from literature (Daniele , 2010), where a large deviation was found in comparison to the experimental measurements, which is referred to big margins of chemical composition presented in the regression. Another calculation based on correlation between VH hardness values measured at the cross section of the tested bars and the bar Y.S, where a large fluctuation of the results was found, this trial was based on the equations introduced by Monideepa Mukherje et al.(2012). Therefore, it is decided to derive a regression relation for the present actual case, based on data collected from both production line and laboratory. To apply precisely the ROM, the Tempcore treated bar, is divided in a

series of concentric tubes with varied yield strength. This is an assumption, since the variation in the structure from the bar centre to its periphery is gradual. Thus, for applying ROM, the additively yield strengths of the two main inner cylinder with pearlite and ferrite and the outer shell tube (layer) with martensite is considered. Tensile specimens for each zone of these two zones were cut from Tempcore bars representing different tempering temperature, while the zone thickness was defined by microscopic observations and hardness test. The diameter of the tensile specimen depended on the zone thickness. Figures 7 and 8 show the microstructure and micro hardness of a 16 mm bar. As expected, the hardness at the center of the rebar is the lowest 188 VH and it increases with increasing distance from the center up to 290 VH, which is due to the microstructure change across the bar cross section ferrite- pearlite core, transient zone and tempered martensite surface layer. The as hot rolled bar yielded almost constant hardness average value of VH 180, throughout the cross section due to its homogenous ferrite-pearlite microstructure.

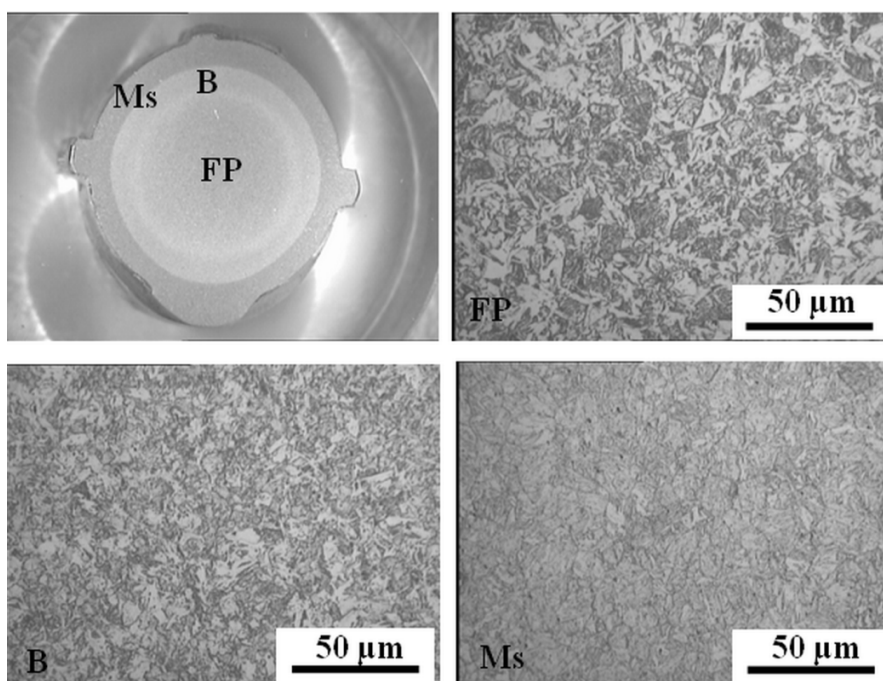


Fig.7: typical microstructure variation in cross section of Tempcore treated bar 16 mm, ferrite-pearlite core, transient zone and tempered martensite surface layer.

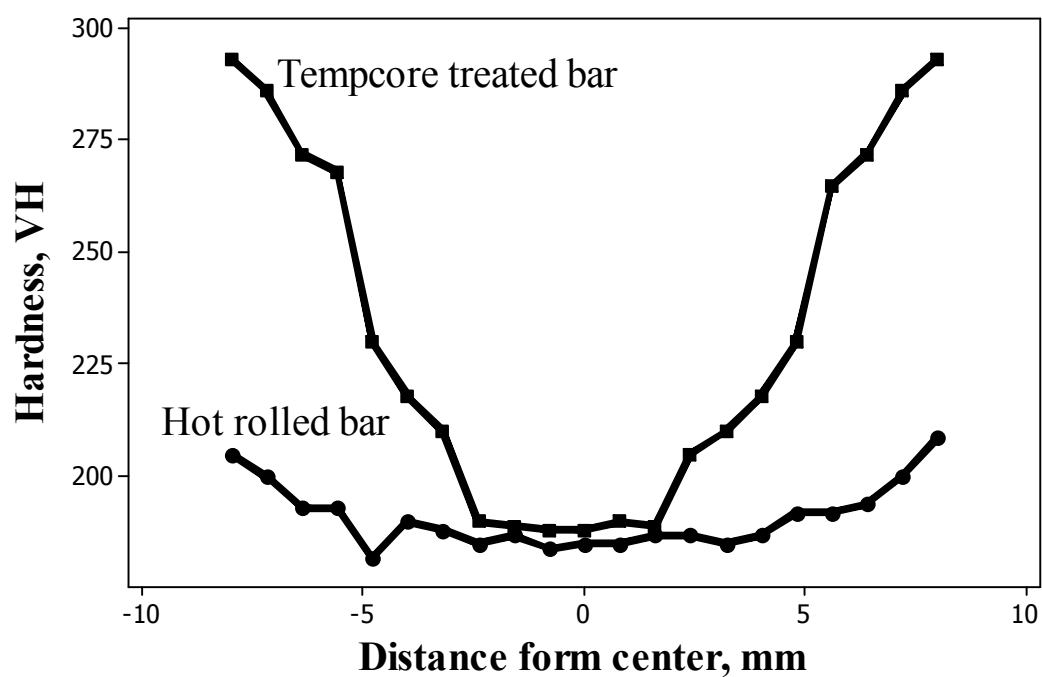


Fig.8: Typical hardness profiles along a diameter of normalized bar and tempcore treated bar

In accordance with this approach, Y.S. corresponding to different tempering temperature is determined and a regression analysis was applied to the results as shown at figure 9, the resulted equation from regression is:

$$Y.S_{core} = 0.0045TT^2 - 5.7766TT + 2222 \quad 21$$

To obtain tempcore treated bars wholly with martensite, they were hold inside the quenching box and then tempered isothermally inside furnace at average temperatures from 540 to 650 °C, and then air cooled. Tensile test was carried out for the tempered martensite samples and the regression was carried out for the data presented in figure 9, as described by the following equation:

$$Y.S_{Ms} = 0.0069TT^2 - 9.9486TT + 4232 \quad 22$$

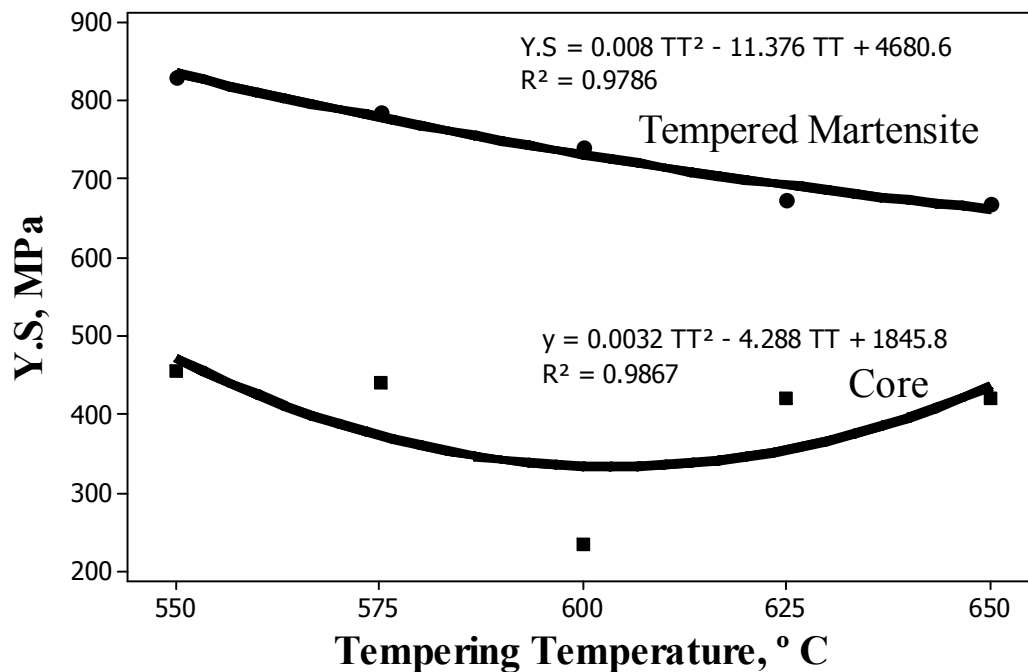


Fig.9: regression curve link the yield strength of Tempered martensite and ferrite-pearlite core, with the Tempering temperature.

4.7. Input parameters into the model

Table 2: lists the input parameters of the model, organized by user and program defined parameters, as well as by parameter type. In addition to the input parameters listed here, various characteristics of the program can also be defined based on user selection. This group of characteristics allows the user to customize the output of the program and to define what type of analysis to perform. However, since the fundamental behavior of the model is not affected, they are not included here.

Table2. Input parameters to the computer model.

	User Defined		Internal to Program
General Parameters	Bar diameter (R)	To be inserted at each model run (mm)	
	Bar initial temperature	To be inserted at each model run (° C)	
	Water Temperature (T_w)	To be inserted at each model run , if not inserted the default 25°C	
	Air Temperature T_a	To be inserted at each model run , if not inserted the default 25°C	
	Total water flow rate	To be inserted at each	

		model run (m^3/h)	
	Water pressure	To be inserted at each model run (bar)	
	Number of cooling nozzles	To be inserted at each model run	
	Length of cooling nozzle	To be inserted at each model run (m)	
	Pipe radius (R_c)	To be inserted at each model run (mm)	
			Quenching time
			Air cooling time till achieving equalizing Temperature
			Heat transfer coefficient of water h_w
Model Parameters	Number of nodes in R direction(M)		Distance increment in r direction Δr
			Time stability Δt
Material Properties			Density (ρ_s) = 7850 (kg/m^3)

Steel			C_P and $K=a+bT+cT^2$ Where, T is temperature in K, and a, b and C are constants
Physical Properties Of Water	Density (ρ_w)	996 (kg/m^3)	
	Dynamic viscosity (ϑ_w)	9.93×10^{-5} ($kg/m \cdot sec$)	
	Prandtle number (Pr)	7	
	Thermal conductivity (k_w)	0.597 ($w/m \cdot C$)	
Physical Properties Of Air	Thermal conductivity (k_a)	0.0255 ($w/m \cdot C$)	
Isothermal Data			Ar1
			Ar3
			Martensite start and finished temperature

▪ **Isothermal Data**

Phase transformation temperatures: Ar1, Ar3 were calculated according to the following equations. (Allen, 2010).

$$A_{r3} = 910 - 273 C - 74 Mn - 56 Ni - 16Cr - 9 Mo - 5 Cu \quad 23$$

$$A_{r1} = 706.4 - 350C - 118.2 Mn \quad 24$$

Where:

Ar3: Start Temperature of the Transformation Austenite to Ferrite [°C]

Ar1: Final Temperature of the Transformation Austenite to Ferrite [°C]

Alloy Content: [weight %].

5. Results and discussion

Overall yield strength of Tempcore treated bars depends on, the volume fraction (percentage) of martensite outer shell zone and the yield strengths of martensite and of the ferrite-pearlite core. The volume percentage of martensite layer depends on the starting temperature of martensite transformation, chemical composition and the cooling parameters during the quenching stage. Yield strength of the martensite layer depends on the chemical composition and the tempering temperature TT. Yield strength of the core depends on the chemical composition and the cooling conditions of the quenching device. For a certain chemical composition and a start quench temperature, the final yield strength of tempcore treated bars depends on the martensite volume fraction and the tempering temperature; both M_s $V_f\%$ and TT being depending on cooling water flow rate and quenching time. Figure 10 shows the effect of cooling water flow rate Wfr on tempering temperature TT for sizes of 10 and 16 mm. For size 10 mm rolling temperature is 1000°C, quenching time 0.4 Sec, rolling speed 14 m/sec and cooling length is 5.7 m. For size 16 mm rolling temperature is 1000°C, quenching time 1.1 Sec, rolling speed 6.2 m/sec and cooling length is 6.87 m. The figure reflects that increasing cooling water flow rate Wfr results in decreasing the tempering temperature TT. For size of 16 mm; water flow rate was varied 120 m³/h to 200m³/h resulting in decreasing tempering

temperature TT from 680 to 550° C. For size 10 mm when the water flow rate varied from 80 m³/h to 120 m³/h, TT decreased from 6000°C to 480 °C.

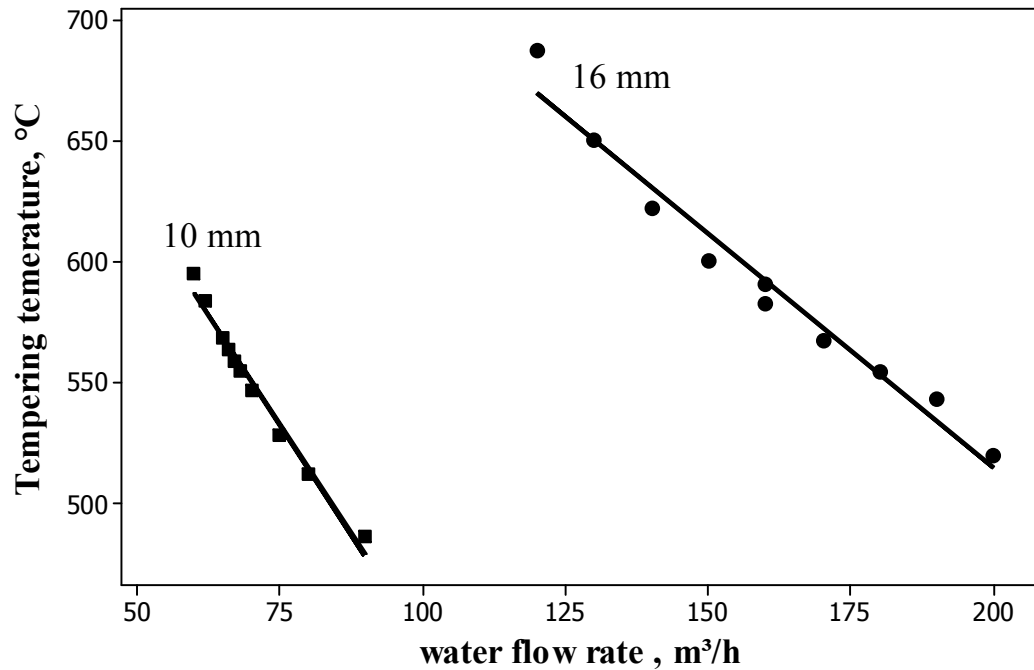


Fig.10: Effect of cooling water flow rate on tempering temperature.

Variation of TT with quenching time Q_t for bar diameters of 10 and 16 mm is shown in fig.11. It should be noted that the relation between the quenching time and tempering temperature is linear with increasing Q_t , TT decreases. This could be explained since increasing quenching time means that the contact time between the cooling water and the quenched bar increases. Therefore the chance to remove more heat from the bar increases leading to less temperature in the surface nodes and the heat losses by conduction inside the bar increases also leading to drop in the temperature at which the equalization between core and surface occurs. It is also noticed that the slop of curve increases sharply with decreasing the diameter. This

required more process construability when applying the quenching process for smaller bar diameters.

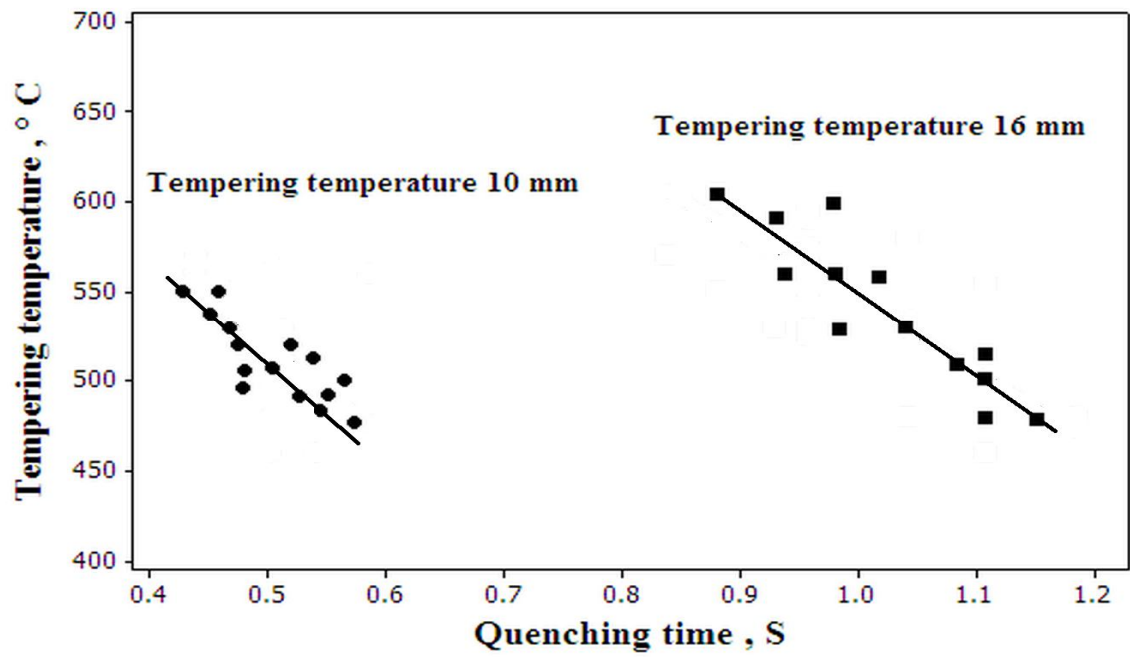


Fig.11: Effect of quenching time on the tempering temperature.

Tempering temperature and martensite volume fraction are the controlling factors of yield strength. This is shown in figure 12, which shows the relation between both of them for bar diameters 10 and 16mm, with initial quenching temperature 1000°C and carbon equivalent 0.41. Figure 13 shows that decreasing tempering temperature by the mean of increasing quenching water flow rate or increasing quenching time is a good control factor to get the desired yield strength.

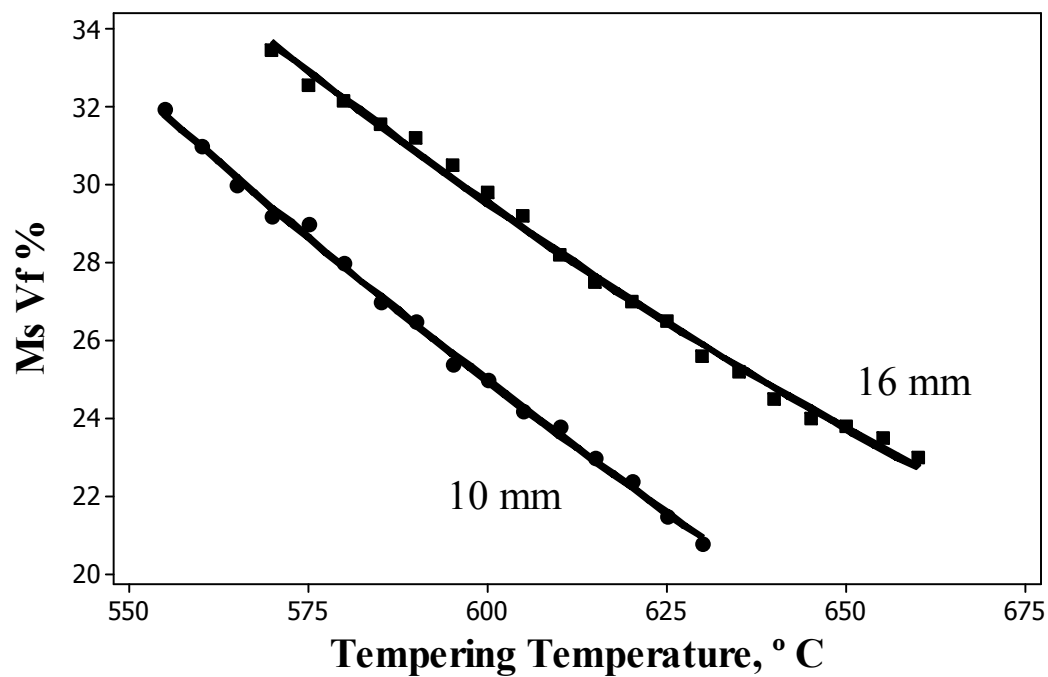


Fig.12: Effect of Tempering Temperature on martensite volume fraction.

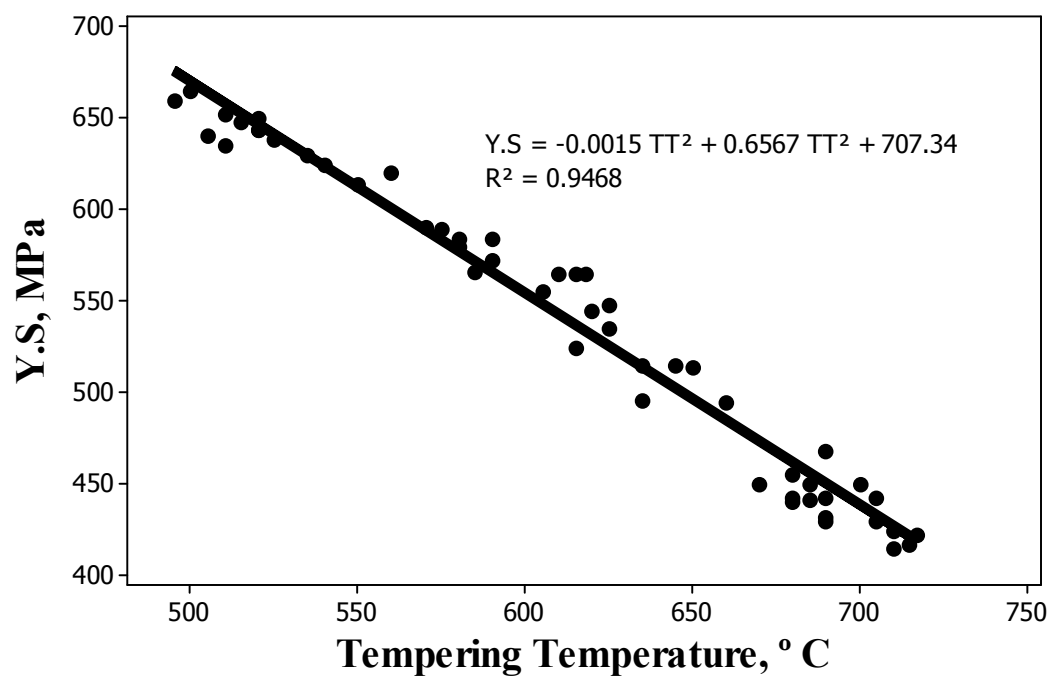


Fig.13: Effect of Tempering Temperature on yield strength.

6. Model Validation

Model output parameters were validated against actual measurements namely; the distribution of the temperature across the radius of the bar at the end of quenching line, Martensite volume fraction, Tempering temperature TT, bar yield strength and the effect of different independent parameters such as cooling time, water flow rate, bar initial temperature, bar size, cooling pipe length and diameter on the process output. The values of the bar and the Tempcore process parameters were combined with each other, and based on finite difference program was run to give the results. 200 runs were done using different cooling water flow rate and quenching time for bar diameters of 10 and 16mm. The run results were compared with the results from the in plant trials to validate the model outputs parameters namely, martensite volume fraction Ms Vf% , tempering temperature TT and yield strength.

6.1. Validation of MsVf %.

MINITAB, (16 VTM) statistical analysis software, is used to compute the regression coefficients to check whether the fitted model actually describes the experimental data. The regression coefficient (R-square) is computed for the martensite volume fraction Ms Vf% and is found to be 92.45%. This reflects that the model can explain the variation in the martensite volume fraction up to the extent of 92.45%. Fig.14 shows the graphical comparison of predicted values of Ms Vf% versus the measured values for 30 runs selected to cover wide range of process parameter, tables 3 and 4 shows respectively the dimensions of the cooling nozzles and the quenching parameters applied in the present work.

Table 3. Dimensions of the cooling nozzles

Set number	Nozzle length, mm	nozzle diameter, mm
10	1404	20.4
16	1374	28

Table 4 : process parameters for both sizes 10 and 16 mm.

Carbon equivalent	Bar diameter, mm	No. of cooling nozzles	Length of cooling nozzle mm	Cooling length, m	Cooling time, s	Water flow rate, m ³ / h	Rolling finishing temp.,
0.399–0.418	10–16	3–7	1374–1404	4.122–9.828	0.35–2.2	90–300	1000

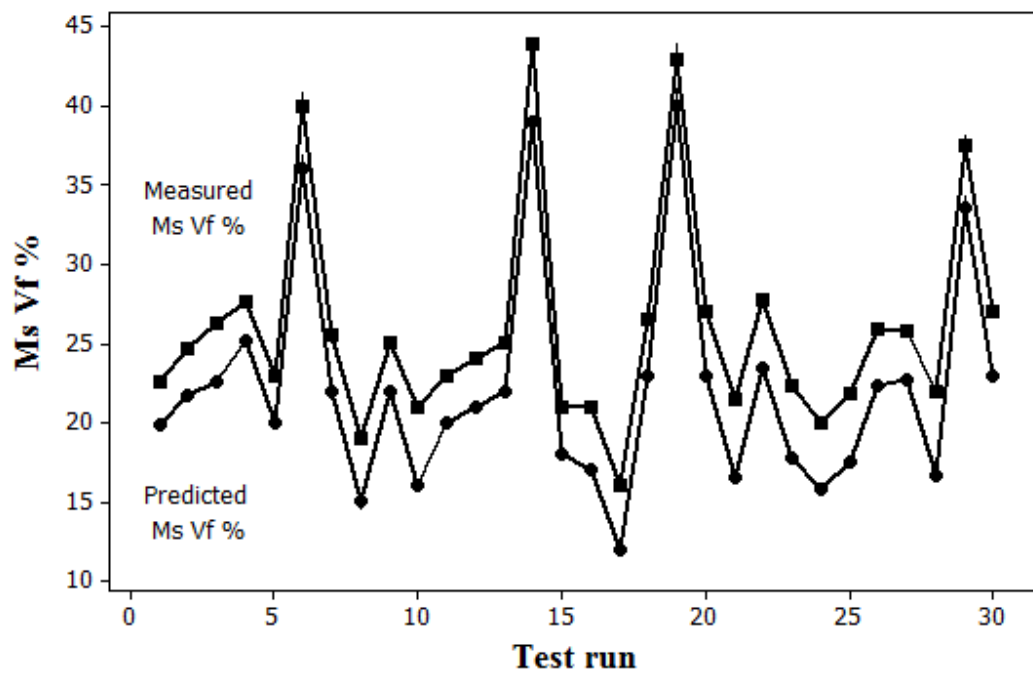


Fig.14: Comparison of predicted MsVf% versus measured values.

6.2. Validation of TT.

From the MINITAB, (16 V) statistical analysis software, the computed regression coefficient (R-square) for the tempering temperature TT is found to be 91% . This

reflects that the model can explain the variation in the tempering temperature up to the extent of 91%. Fig.15 shows the graphical comparison of predicted values of Ms Vf% versus the measured values.

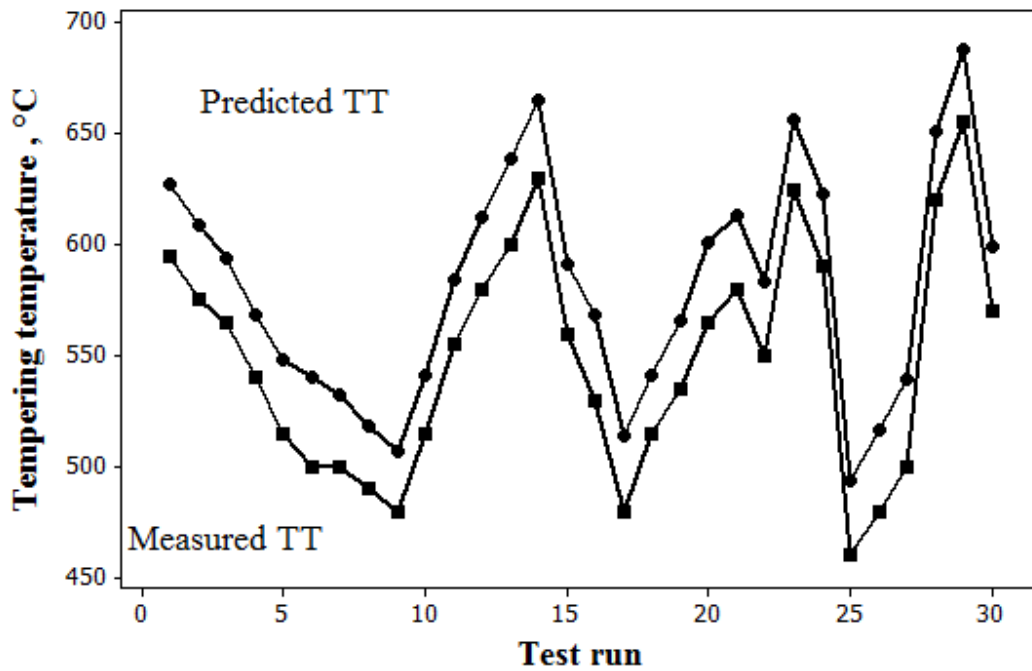


Fig.15: Comparison of predicted tempering temperature versus measured values.

6.3. Validation of Y.S

The regression coefficient (R-square) for the yield strength is found to be 88.4%. This shows that the model can explain the variation in the yield strength up to the extent of 88.4%. Fig.16 shows the graphical comparison of predicted values of Y.S versus the measured values.

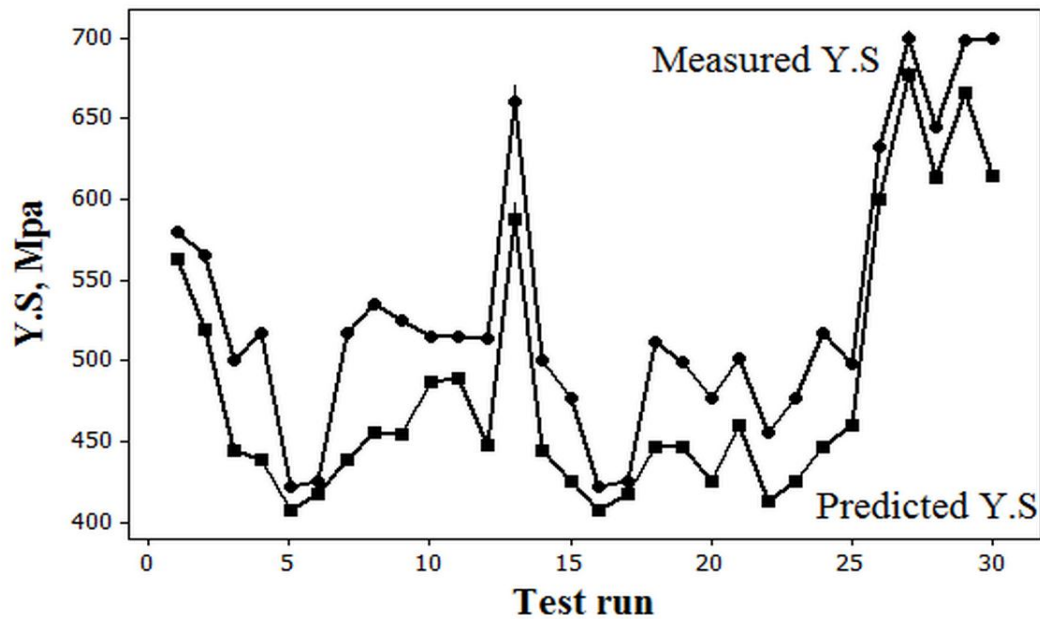


Fig16: Comparison of predicted Y.S versus measured values.

7. Conclusions:

- Controlling the quenching parameters resulted in change of yield strength from 400 to 7000 MPa for a certain chemical composition and quenching start temperature.
- For a certain quenching start temperature and chemical composition, tempcore process could be precisely controlled through changing the main process parameters, namely, water flow rate and quenching time.
- Determination of tempering temperature, volume percentage of internal structures and yield strength has been predicted by finite difference model. The program was practically validated by different experimental inputs of a steel plant.
- The model is useful to determine the cooling box parameters in the tempcore process, without conducting experimental work avoiding material and time waste.

References

- Allen,M.,2011.An Investigation of the Suitability of Using AISI 1117 Carbon Steel in a Quench and Self-Tempering Process to Satisfy ASTM A 706 Standard of Rebar. M.Sc. Thesis. University of Toronto, Canada.
- Bala,P., 2009. Tempcore process analysis based on the kinetics of phase transformations.Archive of metallurgy and metals. 54,1223-1230.
- Çetinel,H .,Toparli,M.,Özsoyeller, L . 2000. A finite element based prediction of the Microstructural evolution of steels subjected to the Tempcore process. Mechanics of Materials 32 , 339-347.
- DANIELI manuals,2010. EZZSTEEL bar mill contract .
- Denis, S.,Farias,D .,Simon,A .1992. Mathematical model coupling with phase transformation and temperature evolution in steel. ISIJ,32.316-325.
- Economopoulos, M., Respen, Y., Lessel, G., Steffes, G., 1975.Application of the tempcore process to the fabrication of high yield strength concrete-reinforcing bars. CRM Report 45, 1-17.

Hazem, L.1997. Modeling of microstructure evolution and properties during cooling of hot rolled steel wire rod. M.Sc. Thesis University of London, Imperial college of science, technology and medicine, department of material, London.

Hollman,J.O .1990. Heat transfer, 7th Edition, McGraw - Hill , New York.

Incropera, F.P, Dewitt, D.P. , 1996 . Introduction to heat transfer, 3rd edition. Wiley, New York

Isukapalli,B. ,Sankar, K. ,Mallikarjuna,R.,Gopala,A., 2010.Prediction of heat transfer coefficient of steel barssubjected to Tempcore process using nonlinear modeling. Int J AdvManufTechnol, 47,1159–1166.

Jacques,H., Boris,D.,2004. MCP application in sections, bars and rails, 2nd international conference on thermomechanical processing of steels, liege, Belgium, 459-466 .

Kang,S.H.,Im, Y.T.,2005. Three-dimensional finite-element analysis of the quenching process of plain-carbon steel with phase transformation, Metallurgical and Materials Transactions.36A, 2315.

Lindemann,A. , Schmidt, J., 2005. ACMOD-2DdA heat transfer model for the simulationof the cooling of wire rod, Journal of Materials Processing Technology169 (2005) 466-475.

Monideepa, M., Chaitali, D., Arunansu, H., 2012. Prediction of hardness of the tempered martensitic rim of TMT rebars. *Materials Science and engineering. A* 543 ,35-44.

Munira, M., Dhindaw B.K., Roy, A., 1994. Modeling of eutectoid transformation in plain carbon steel. *ISIJ*. 34.355-358.

Nobari, A.H., Serajzadeh, S., 2011. Modeling of heat transfer during controlled cooling in hot rod rolling of carbon steels. *Applied Thermal Engineering* 31, 487-492.

Purcell, A. 2000. Mathematical modeling of temperature evolution in the hot rolling of steel. Master of engineering thesis, Department of Mining and Metallurgical engineering, McGill University, Canada.

Prakash, K.A., Brimacombe, J.K., 1981. Mechanical modeling of heat flow and austenite pearlite transformation in eutectoid carbon steel rods for Wires. *Metallurgical transaction*. Vol. 12 B .121-133.

Rodríguez, R., Gutiérrez, I., 2004. Mechanical behavior of steels with mixed microstructures. 2nd international conference of thermomechanical processing of steels, liege, Belgium, 356-363.

Suehiro, M., Senuma, T., Yada, H., Sato, K., 1992. Application of mathematical model for prediction microstructural evolution to high carbon steel”, *ISIJ*. 32, 33-439.

Simon P, Economopoulos, M., Nilles, P., 1984. Tempcore a new process for production of high quality reinforcing bars. *Iron Steel Engineering*. 61(3), 55–57.

Monideepa Mukherjee, Chaitali Dutta, Arunansu Haldar, 2012. Prediction of hardness of the tempered martensitic rim of TMT rebars. *Materials Science and Engineering A* 543, 35–43.

List of tables

Table No.	Captions
Table 1	Chemical composition of the investigated reinforcing steels (mass contents in %).
Table 2	Input parameters to the computer model
Table 3	Dimensions of the cooling nozzles
Table 4	Process parameters for both sizes 10 and 16 mm.

List of figures

Figure No.	Captions
Figure 1	Temperature profile of Tempcore treated bars at the different stages and the corresponding microstructural changes
Figure 2	Relation between the process parameters and the main mechanisms of Tempcore process
Figure 3	One-dimensional heat transfer in infinite cylinder
Figure 4	Discretization of Cylinder
Figure 5	Thermal profile of the bar from the cooling box entering to equalizing temperature normal scale
Figure 6	Thermal profile of a bar at exit from cooling box .
Figure 7	Typical microstructure variation in cross section of Tempcore treated bar 16 mm.
Figure 8	Typical VH profile along a diameter of 16mm normalized bar and 16 mm Tempcore treated bar
Figure 9	Regression curve link the yield strength of tempered martensite and ferrite-pearlite core, with tempering temperature.
Figure 10	Effect of cooling water flow rate on tempering temperature
Figure 11	Effect of quenching time on tempering temperature
Figure 12	Effect of tempering temperature on martensite volume fraction
Figure 13	Effect of tempering temperature on yield strength
Figure 14	Comparison of predicted $M_s V_f\%$ versus measured values
Figure 15	Comparison of predicted tempering temperature versus measured values.
Figure 16	Comparison of predicted Y.S versus measured values

Appendix

Title	Page No.
Abstract	1
Introduction	2
Methodology	4
Experimental work	5
Mathematical model	6
Thermal model	7
Discretization	11
Explicit Form of FDE	12
Stability equations	13
Metallurgical model	14
Mechanical properties model	16
Input parameters to the model	20
Results and discussion	27
Validation of $MsVf\%$	27
Validation of TT	28
Validation of Y.S	29
Conclusions	30
References	31
List of tables	35
List of figures	36
Appendix	37